

Photolysis of Chiral 1-Pyrazolines to Cyclopropanes: Mechanism and Stereospecificity

Elena Muray,[†] Ona Illa,[†] José A. Castillo,[†] Ángel Álvarez-Larena,[‡] José L. Bourdelande,^{*,†} Vicenç Branchadell,^{*,†} and Rosa M. Ortuño^{*,†}

Departament de Química, Universitat Autònoma de Barcelona, 08193 Bellaterra, Barcelona, Spain, and Unitat de Cristal·lografia, Universitat Autònoma de Barcelona, 08193 Bellaterra, Barcelona, Spain

jose Luis.bourdelande@uab.es; vicenc@klingon.uab.es; rosa.ortuno@uab.es

Received February 24, 2003

The photodenitrogenation of chiral trisubstituted 1-pyrazolines has been studied by laser flash photolysis. These experiments have permitted the detection of two transients that have been assigned, for each pyrazoline, to the trimethylene-type diradical resultant from the extrusion of nitrogen (lifetime $\tau = 0.1\text{--}0.8\ \mu\text{s}$) and to the pyrazoline triplet ($\tau < 9\ \text{ns}$), respectively. The efficiency of the photosensitization process has been evaluated by determination of the corresponding quenching rate constant in each instance. Theoretical calculations support a mechanistic pathway involving a trimethylene radical as intermediate that rapidly evolves to the corresponding cyclopropane derivative. The cyclopropane ring-closure is predicted to be faster than rotation around the C–C bond, thus accounting for the observed stereospecificity.

Introduction

The photochemical denitrogenation of 1-pyrazolines is a method extensively used in organic synthesis to prepare cyclopropane derivatives. The mechanism of these reactions has been controversial for long time. At present, it is accepted that these processes generally involve diradicals, although the mode of formation and their structure as singlet or triplet may vary with the substrate and reaction conditions.¹ The presence of a photosensitizer is often required for the reaction to take place efficiently and to avoid the formation of byproducts such as cycloreversion or insertion olefines.^{2,3} This fact suggests that the process occurs via triplet excited states.⁴ Trapping of triplet diradicals has been achieved, indeed, by using stable nitroxides as scavengers⁵ whose efficiency depends strongly on steric and solvent effects,⁶ as well as on the transient lifetimes.

The intermediacy of triplet diradicals has been invoked to explain the low stereoselectivity observed in the photochemical denitrogenation of some diazabicyclo[2.2.1]-heptenes (DBH) to produce housanes.^{4b} The photochemical behavior of DBH derivatives has been rationalized by means of theoretical calculations accounting for the nature of the experimentally observed triplet intermediates.^{7,8}

1-Pyrazolines are currently produced through 1,3-dipolar cycloadditions of diazoalkanes to electron-deficient olefines. When these substrates are chiral, the π -facial diastereoselection of the cycloaddition is responsible for the configuration of the newly created stereogenic centers. If the photolysis of the pyrazolines takes place via open-chain diradicals, it is possible that the cyclopropane ring closure is not stereospecific, so that a mixture of all possible diastereomers would be expected.

In our laboratory, we have performed the highly stereoselective cycloaddition of diazomethane to optically active trisubstituted olefins derived from D-glyceraldehyde⁹ and (–)-verbenone,¹⁰ and we have investigated the origin of the π -facial diastereoselection.^{9,11} Photolysis of

[†] Departament de Química.

[‡] Unitat de Cristal·lografia.

(1) Smith, M. B.; March, J. *Advanced Organic Chemistry*, 5th ed.; J. Wiley & Sons: New York, 2001; p 1353 and references therein.

(2) For some representative works, see: (a) Engel, P. S.; Shen, L. *Can. J. Chem.* **1974**, *52*, 4040. (b) Engel, P. S.; Steel, C. *Acc. Chem. Res. Chem.* **1973**, *6*, 275. (c) Engel, P. S.; Nalepa, C. L. *Pure Appl. Chem.* **1980**, *52*, 2621. (d) Doubleday, C.; McIver, J. W.; Page, M. *J. Am. Chem. Soc.* **1982**, *104*, 6533. (e) Karatsu, T.; Hotta, H.; Kitamura, A. *J. Chem. Soc., Chem. Commun.* **1991**, 1451.

(3) (a) Wilkinson, F.; Kelly, G. P. *J. Photochem. Photobiol., A: Chem.* **1990**, *52*, 309. (b) Wilkinson, F.; Kelly, G. P.; Michael, C. *J. Photochem. Photobiol., A: Chem.* **1990**, *52*, 309. (c) Blair, J. T.; Sahyun, M. R. V.; Sharma, D. K. *J. Photochem. Photobiol., A: Chem.* **1994**, *77*, 133.

(4) See, for instance: (a) Adam, W.; Grabowski, S. *J. Am. Chem. Soc.* **1987**, *109*, 7572. (b) Adam, W.; Garcia, H.; Martí, V.; Moorthy, J. N. *J. Am. Chem. Soc.* **1999**, *121*, 9475. (c) Adam, W.; Martí, V.; Sahin, C.; Trofimov, A. *J. Am. Chem. Soc.* **2000**, *122*, 5002.

(5) See, for instance: Adam, W.; Bottle, S. E.; Finzel, R.; Kammel, T.; Peters, E.-M.; Peters, K.; von Schnering, H. G.; Walz, L. *J. Org. Chem.* **1992**, *57*, 982.

(6) (a) Chateaufeuf, J.; Luszyk, J.; Ingold, K. U. *J. Org. Chem.* **1988**, *53*, 1629. (b) Beckwith, A. L. J.; Bowry, V. W. *J. Org. Chem.* **1988**, *53*, 1632. (c) Beckwith, A. L. J.; Bowry, V. W.; Ingold, K. U. *J. Am. Chem. Soc.* **1992**, *114*, 4983. (d) Bowry, V. W.; Ingold, K. U. *J. Am. Chem. Soc.* **1992**, *114*, 4992.

(7) Robertson, M. J.; Simons, J. *J. Phys. Chem.* **1997**, *101*, 2379.

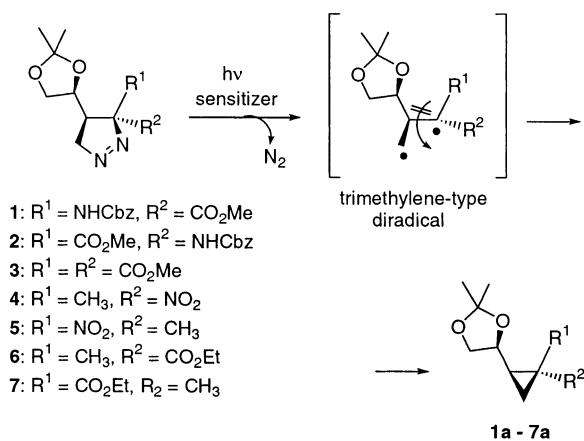
(8) Yamamoto, N.; Olivucci, M.; Celani, P.; Bernardi, F.; Robb, M. A. *J. Am. Chem. Soc.* **1998**, *120*, 2391.

(9) Muray, E.; Álvarez-Larena, A.; Piniella, J. F.; Branchadell, V.; Ortuño, R. M. *J. Org. Chem.* **2000**, *65*, 388.

(10) Moglioni, A. G.; García-Expósito, E.; Álvarez-Larena, A.; Branchadell, V.; Moltrasio, G. Y.; Ortuño, R. M. *Tetrahedron: Asymmetry* **2000**, *11*, 4903.

(11) Illa, O.; Muray, E.; Amsallem, D.; Moglioni, A. G.; Gornitzka, H.; Branchadell, V.; Baceiredo, A.; Ortuño, R. M. *Tetrahedron: Asymmetry*, **2002**, *13*, 2593.

SCHEME 1



the resultant pyrazolines has been shown to be stereospecific (Scheme 1) allowing the preparation of cyclopropane derivatives used as synthetic precursors to a variety of products such as conformationally constrained amino acids^{10,12} and peptides,¹³ amino alcohols,¹⁴ and cyclopropane carbocyclic nucleosides.¹⁵ In a previous paper, we studied the photophysics of two diastereomeric pyrazolines and their stereospecific denitrogenation to the corresponding cyclopropanes. We suggested therein that the pyrazoline decomposition takes place by nitrogen extrusion with the concomitant production of a trimethylene-type diradical, in such a way that cyclopropane ring-closure should be faster than rotation around the C–C bond.¹⁶

In this work, we extend this study to other trisubstituted 1-pyrazolines in order to detect and characterize the transients involved in the process and to determine the efficiency of the photosensitizers by means of laser flash photolysis (LFP) experiments. Theoretical calculations have been done to account for the more favorable mechanistic pathway, for the nature of the transient intermediates, and to explain the observed stereospecificity.

Results and Discussion

1. Photolysis of the Pyrazolines. For this study, we have chosen pyrazolines **1–7** (Scheme 1) that were synthesized through the 1,3-dipolar cycloadditions of diazomethane to suitable olefins prepared, in turn, from D-glyceraldehyde acetonide.⁹ Pyrazoline **3** was prepared and characterized for the first time in this work, and its stereochemistry was unambiguously assigned by X-ray diffraction analysis (see the Supporting Information).

(12) (a) Jiménez, J. M.; Rifé, J.; Ortuño, R. M. *Tetrahedron: Asymmetry*, **1996**, *7*, 537. (b) Jiménez, J. M.; Ortuño, R. M. *Tetrahedron: Asymmetry*, **1996**, *7*, 3203. (c) Rifé, J.; Lajoie, G. A.; Ortuño, R. M. *J. Org. Chem.* **1999**, *64*, 8958. (d) Illescas, B.; Rifé, J.; Ortuño, R. M.; Martín, N. *J. Org. Chem.* **2000**, *65*, 6246.

(13) (a) Díaz, M.; Jiménez, J. M.; Ortuño, R. M. *Tetrahedron: Asymmetry*, **1997**, *8*, 2465. (b) Martín-Vilà, M.; Muray, E.; Aguado, G. P.; Alvarez-Larena, A.; Branchadell, V.; Minguillón, C.; Giralt, E.; Ortuño, R. M. *Tetrahedron: Asymm.* **2000**, *11*, 3569.

(14) Rifé, J.; Ortuño, R. M. *Tetrahedron: Asymmetry* **1999**, *10*, 4245.

(15) Muray, E.; Rifé, J.; Branchadell, V.; Ortuño, R. M. *J. Org. Chem.* **2002**, *67*, 4520.

(16) Jiménez, J. M.; Bourdelande, J. L.; Ortuño, R. M. *Tetrahedron* **1997**, *53*, 3777.

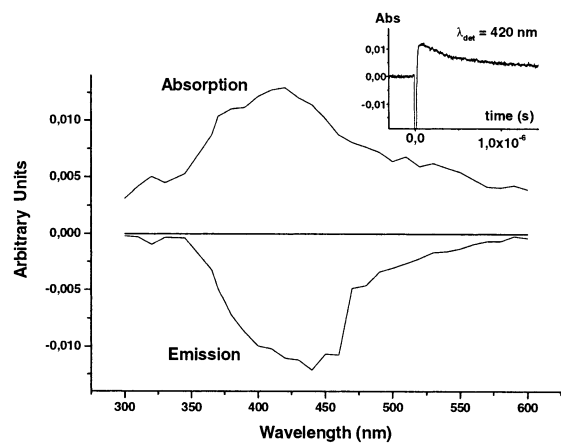


FIGURE 1. Transient absorption and emission spectra ($\lambda_{\text{ex}} = 355$ nm, 40 mJ/pulse, 9 ns width) of a nitrogen-purged dichloromethane solution of pyrazoline **3**. Inset: decay trace at 420 nm.

Under stationary irradiations, pyrazolines **1–7** afforded the corresponding cyclopropanes **1a–7a** with total stereospecificity.^{9,16} The pyrazoline solutions, contained in Pyrex reactors, were irradiated with a 125 W medium-pressure mercury lamp. For **4** and **5**, acetone was used both as sensitizer and solvent. In the other cases, benzophenone was the sensitizer and dichloromethane was the solvent. Yields were excellent for the decomposition of **1–3** and **6–7** (88–100%) and moderate (46–52%) for **4–5**. In the latter cases, yield was lower (ca. 35%) when benzophenone was used as sensitizer. These results are probably due to the lability of the nitro group under the reaction conditions leading to the production of unidentified photoproducts.

Attempts to trap the postulated intermediate diradicals failed, since the addition of dimethyl acetylene dicarboxylate or TEMPO did not result in the formation of defined products. Nevertheless, is noteworthy that, when the photolysis of **7** was performed in the presence of Tempo, the corresponding cyclopropane was obtained in only 40% yield (cf. 90% yield under the usual conditions) along with much polymeric material. The steric hindrance of the tertiary-carbon radical could avoid the interaction with the scavenger that would react only with the primary-carbon radical, thus accounting for the formation of undefined substances.

LFP experiments were carried out to verify the nature of the transient species and to state the role of the sensitizers. Since the ground-state UV absorption spectra of pyrazolines show a band corresponding to an $n-\pi^*$ transition that maximizes at 320–330 nm, compounds **1–3** and **7** were irradiated, as degassed dichloromethane solutions, with 355 nm laser pulses of 40 mJ (9 ns/pulse width) and their transient absorption spectra were recorded. Figure 1 shows the transient spectra obtained for **3** as well as the deactivation decay profile at 420 nm. This decay shows an emission signal that quickly builds up a positive transient absorption following the kinetics of the laser pulse profile. As a consequence, we can only state that the transient species responsible for the emission has a lifetime $\tau < 9$ ns and a transient emission spectrum deduced by global analysis that maximizes at 440 nm. The positive part of the decay follows a deactivation

TABLE 1. Decay Rate Constants^a and Lifetimes^b of the Pyrazoline Transients

pyrazoline	k_d	τ
1 ^c	8.3×10^6	0.1
2 ^c	3.8×10^6	0.3
3	2.0×10^6	0.5
7	1.2×10^6	0.8

^a In s⁻¹. ^b In μ s. ^c Reference 16.

TABLE 2. Benzophenone Quenching Rate Constants^a by Pyrazolines

pyrazoline	k_q
1 ^b	1.7×10^9
2 ^b	1.2×10^9
3	1.8×10^9
4	3.9×10^5
7	1.2×10^9

^a In s⁻¹ mol⁻¹ dm³. ^b Reference 16.

tion with a rate constant $k_d = 2.0 \times 10^6$ s⁻¹ corresponding to a deduced lifetime $\tau = 0.5$ μ s. Finally, a flattened decay was also observed at longer times. Table 1 shows also the decay constants for pyrazolines **1**, **2**, and **7** deduced in a similar way by using the global analysis.

In an earlier work,¹⁶ we assigned these positive absorptions to transients corresponding to the pyrazoline triplet and the diradical resultant from extrusion of nitrogen prior to the cyclopropane ring-closure. The latter detection of the transient species responsible for the emission led us to a reassignment. Thus, we now suggest that the trimethylene-type diradical, in each case, corresponds to transients listed in Table 1, with lifetimes between 0.1 and 0.8 μ s while transients living <9 ns should be the pyrazoline triplets.

In a similar manner, k_d for the benzophenone triplet was determined from the mono exponential decay of its transient and found to be 5.5×10^5 s⁻¹. Moreover, the addition of amounts of a determined pyrazoline to the benzophenone containing solution resulted in the disappearance of the sensitizer transient-absorption centered at 530 nm parallel to the appearance of a weak absorption in the 390–450 nm interval. The quenching rate constant (k_q) for pyrazolines **1–4** and **7** were determined from the respective Stern–Volmer graphs and are listed in Table 2. The values of k_q , which is a quantitative measure of the efficiency of the photosensitization process, are similar for all pyrazolines except **4**, in good agreement with the results of stationary irradiations.

Then, the results of all these experiments point out the feasibility of the production of triplet diradicals during the photodecomposition of the pyrazolines to afford cyclopropanes.

2. Theoretical Calculations

We have studied the photodenitrogenation of pyrazoline **4**, due to the simplicity of the nitro and methyl groups compared to the ester groups present in the other pyrazolines. The calculations have been focused in the nitrogen elimination pathway, and the results are expected to be valid for all pyrazolines considered in the previous section.

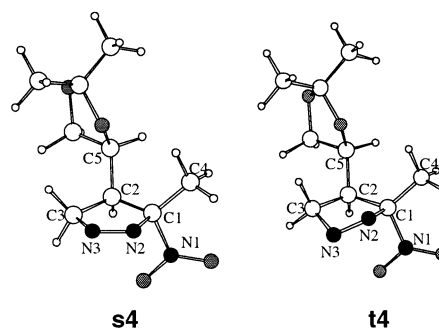
**FIGURE 2.** Structure of the ground state (**s4**) and first triplet excited state (**t4**) of pyrazoline **4**.

Figure 2 shows the structures of the pyrazoline in its ground state, **s4**, and in the first triplet excited state, **t4**. The values of selected geometry parameters are presented in Table 3, and atomic spin populations derived from the Mulliken population analysis are presented in Table 4.

When going from **s4** to **t4** the pyrazoline ring loses its planarity. Moreover, we can observe a lengthening of the C3–N3, N2–N3, and C1–C2 bonds and a shortening of C1–N2. On the other hand, the orientation of the dioxolane ring does not change upon excitation.

t4 corresponds to the mixed $n-\pi^*/\pi-\pi^*$ triplet state described by Yamamoto et al.⁸ The unpaired electrons are located in the pyrazoline nitrogen atoms (see Table 4). The C1–N2 bond distance is notably shorter than the C3–N3 one. However, the cleavage of C1–N2 is energetically more favorable. This process leads to the formation of the diazenyl diradical **t8** with a Gibbs activation energy of 5.3 kcal mol⁻¹. The structures of the stationary points corresponding to the nitrogen elimination from **t4** are shown in Figure 3. Their relative energies, Gibbs energies, as well as values of selected geometry parameters have been included in Table 3, and atomic spin populations are shown in Table 4. At the transition state **TS(t4–t8)** the unpaired electrons are mainly located at the C1, N2, and N3 atoms, whereas for **t8** the atomic spin population on N3 is drastically reduced. The cleavage of the C1–N2 bond makes the rotation around the C1–C2 bond possible, as we can observe from the variation of the ϕ dihedral angle. In this way, steric repulsion between methyl and dioxolane groups is minimized.

The cleavage of the second C–N bond (C3–N3) leads to the formation of the trimethylene diradical **t9** with a potential energy barrier of 1.4 kcal mol⁻¹ and a Gibbs activation energy of only 0.4 kcal mol⁻¹. For this reason, **t8** is expected to be an intermediate with a very short lifetime. In **t9**, we can observe a stabilizing interaction involving the C5 hydrogen atom and the nitro group with an O–H distance of 2.64 Å.

t9 may evolve to the singlet potential energy surface and then to the cyclopropane product. This process competes with the conformational rearrangement associated to the rotation around the C1–C2 bond to form **t9'**. The structures of **t9'** and the conformational transition state are shown in Figure 4, and their energies and geometrical parameters have been included in Table 2. The computed energy barrier associated to this process is 8.2 kcal mol⁻¹, and the reaction energy is 2.5 kcal mol⁻¹. The imaginary frequency of the transition state

TABLE 3. Relative Energies,^a Gibbs Energies^a at 1 atm and 298.15 K, and Selected Geometry Parameters^b for the Stationary Points^c Corresponding to Nitrogen Elimination from Pyrazoline 4

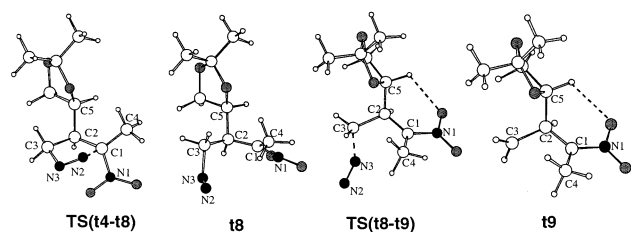
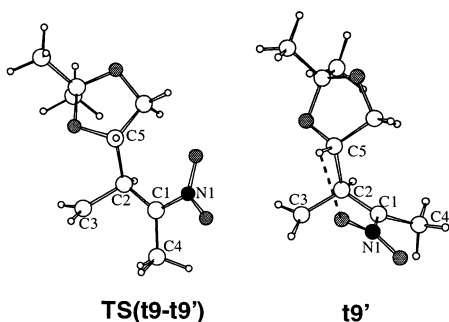
	ΔE	ΔG	C1–N2	C3–N3	C1–C2	C2–C3	N2–N3	ϕ^d
s4	–52.0	–49.7	1.54	1.48	1.55	1.55	1.24	–9.0
t4	0.0	0.0	1.48	1.58	1.59	1.57	1.28	–7.2
TS(t4–t8)	5.9	5.3	1.86	1.51	1.55	1.57	1.22	–1.1
t8	–12.0	–15.7	3.61	1.54	1.50	1.54	1.19	89.4
TS(t8–t9)	–9.8	–15.3	3.80	1.82	1.50	1.52	1.16	89.9
t9	–23.9	–40.5			1.51	1.50		92.4
TS(t9–t9')	–15.7	–31.7			1.51	1.51		162.5
t9'	–21.4	–38.1			1.50	1.50		–115.3

^a In kcal mol^{–1}. ^b Interatomic distances in Å and dihedral angle in deg. ^c See Figures 2–4. ^d C4–C1–C2–C5 dihedral angle.

TABLE 4. Atomic Spin Populations for the Stationary Points^a Corresponding to Nitrogen Elimination from Pyrazoline 4

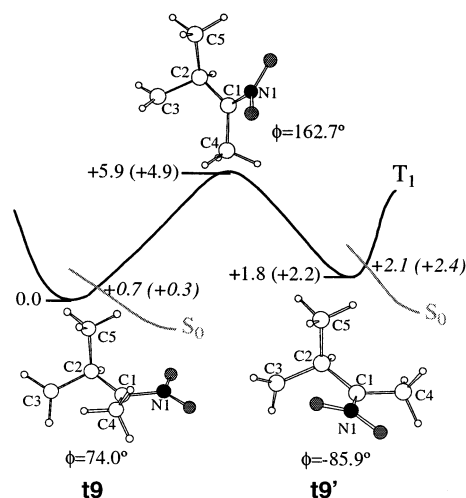
	C1	C3	N2	N3	NO ₂
t4	0.087	0.073	0.722	0.847	0.155
TS(t4–t8)	0.417	0.128	0.625	0.532	0.262
t8	0.736	0.168	0.677	0.145	0.226
TS(t8–t9)	0.733	0.503	0.463	0.057	0.228
t9	0.748	1.071			0.262
TS(t9–t9')	0.734	1.073			0.246
t9'	0.710	1.096			0.226

^a See Figures 2–4.

**FIGURE 3.** Structure of the stationary points corresponding to nitrogen elimination from pyrazoline 4 in the first triplet state.**FIGURE 4.** Structure of the stationary points corresponding to conformational rearrangement of **t9**.

corresponds to a rotation around C1–C2 bond coupled with a rotation of the dioxolane group around the C2–C5 bond. In this way, **t9'** is also stabilized through an interaction between C5–H and the nitro group, the O–H interatomic distance being 2.42 Å. At the transition state **TS(t9–t9')**, the dioxolane and nitro groups are eclipsed. We have also located a transition state structure in which the dioxolane and methyl groups are eclipsed, but it is 2.4 kcal mol^{–1} higher in energy than **TS(t9–t9')**.

Rotation around C1–C2 is hindered due to steric repulsion between dioxolane and nitro or methyl groups.

**FIGURE 5.** Schematic representation of the potential energy surfaces for the T₁/S₀ deactivation and conformational rearrangement of model trimethylene diradical obtained at the CASSCF level of calculation. Relative energies are in kcal mol^{–1}. ϕ is the C4–C1–C2–C5 dihedral angle.

In contrast, rotation around C2–C3 is much easier. We have located the transition state corresponding to this process and the computed energy barrier is only 2.0 kcal mol^{–1}.

The **t9'** conformer would also be produced in the nitrogen elimination from pyrazoline 5, resulting from the addition of diazomethane to the *Z* isomer of the olefin. If conformational rearrangement is faster than cyclopropane ring-closure, the latter process would not be stereospecific.

We have studied the competition between these two processes for a model system in which the dioxolane group has been replaced by a methyl. For this system, we have optimized the geometries of the two conformers **t9** and **t9'** and of the conformational transition state at the CASSCF level of calculation. Moreover, we have located two minimum energy-crossing points between triplet and singlet states in the vicinity of each minimum. The energies of all these structures have also been calculated at the BPW91 level of calculation. The results are summarized in Figure 5. We can observe that **t9** is the most stable conformer and that its rearrangement to **t9'** involves an energy barrier of 5–6 kcal mol^{–1} depending on the level of calculation. These values are about 2–3 kcal mol^{–1} smaller than the value calculated for the real system (8.2 kcal mol^{–1}). The triplet–singlet crossing points are very close to the energy minima and

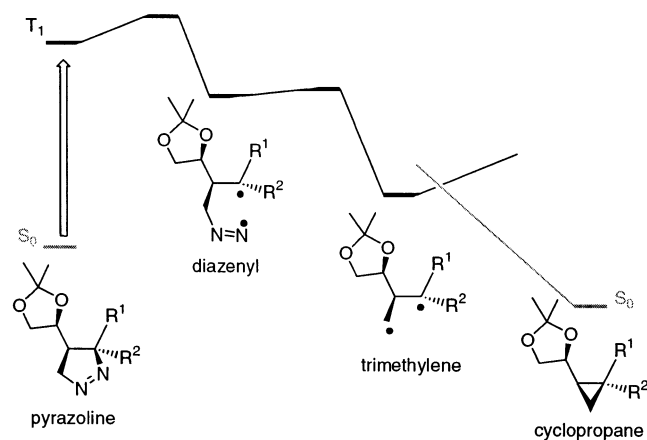


FIGURE 6. Schematic representation of the potential energy surface for the nitrogen elimination from a chiral 1-pyrazoline.

the energy necessary to reach them is much smaller than the conformational potential energy barrier. The energies of the crossing points computed at the BPW91 level of calculation are very similar to the CASSCF energies.¹⁷

At the geometry of the minimum of the triplet **t9**, the singlet is 0.7 kcal mol⁻¹ higher in energy at the CASSCF level of calculation. When the geometry of the singlet is allowed to relax the system evolves toward the corresponding cyclopropane.

At the crossing point close to **t9** the spin-orbit coupling constant is 0.3 cm⁻¹. For parent trimethylene it has been shown that spin-orbit coupling constant has the largest value when both terminal methylene groups are in a face to face arrangement.¹⁸ We have performed a restricted optimization at the CASSCF level of calculation of a structure for **t9** in which the N1-C1-C2-C3 dihedral angle is 90° and one of the H-C3-C2-C1 dihedral angles is -90°. This structure is 2.6 kcal mol⁻¹ above the minimum of **t9**, and the computed spin-orbit coupling constant is 1.1 cm⁻¹. At this geometry, the singlet is 3.1 kcal mol⁻¹ lower in energy than the triplet. The energy necessary to reach this structure is notably lower than the conformational potential energy barrier.

These results suggest that intersystem crossing to the ground-state potential energy surface is faster than the conformational rearrangement, so that the formation of cyclopropane is stereospecific.

Concluding Remarks

The intermediacy of trimethylene-type diradicals in the photodenitrogenation of chiral 1-pyrazolines to cyclopropanes has been evidenced. The stereospecificity observed in these processes can be explained on the basis of theoretical calculations. Thus, starting from the triplet pyrazoline the cleavage of one of the C-N bonds leads to the formation of a diazenyl diradical (Figure 6). The Gibbs activation energy of 5.3 kcal mol⁻¹ computed for pyrazoline **4** is compatible with a lifetime lower than 0.9 ns. The cleavage of the second C-N bond is expected to

be very fast, so that the diazenyl diradical cannot be detected with our present equipment. This process leads to the formation of a trimethylene diradical. Intersystem crossing to the ground state leads to the formation of the corresponding cyclopropane. This process is faster than rotation around a C-C bond, so that the reaction is stereospecific.

Experimental Section

Materials. Pyrazolines **1–7** were prepared as previously described.⁹ (4*S*,4'*S*)-4-(2',2'-dimethyl-1',3'-dioxolan-4'-yl)-3,3-bis(methoxycarbonyl)-1,2-pyrazoline, **3**, is a new product whose configuration was determined by X-ray analysis (see the Supporting Information). Physical constants and spectroscopic data of **3** follow.

Pyrazoline 3: crystals; mp 95–97 °C (from CH₂Cl₂/pentane); [α]_D -228.3 (*c* 1.03, CHCl₃); ¹H NMR (CDCl₃) δ 1.24 (s, 3H), 1.33 (s, 3H), 2.87 (m, 1H), 3.63 (dd, *J* = 8.1 Hz, *J* = 6.3 Hz, 1H), 3.76 (s, 3H), 3.87 (s, 3H), 4.03 (complex absorption, 2H), 4.56 (dd, *J* = 18.1 Hz, *J* = 7.7 Hz, 1H); ¹³C NMR (CDCl₃) δ 25.02, 40.98, 53.23, 53.90, 68.27, 73.22, 79.22, 100.45, 109.46, 165.00, 166.03.

Cyclopropane 3a. Obtained from photolysis of pyrazoline **3** in the usual way.⁹ This compound also resulted from LFP of **3**: oil; [α]_D -15.38 (*c* 0.26, CH₂Cl₂); 250-MHz ¹H NMR (CDCl₃) δ 1.30 (s, 3H), 1.41 (s, 3H), 1.51–1.62 (m, 2H), 1.98 (m, 1H), 3.69 (s, 3H), 3.71 (m, 3H), 3.69–3.81 (m, 2H), 4.07 (dd, ²*J* = 8.0 Hz; ³*J* = 5.7 Hz, 1H); 62.5-MHz ¹³C NMR (CDCl₃) δ 18.67, 25.50, 26.60, 29.84, 52.72, 52.86, 69.16, 75.43, 81.24, 109.45, 168.03, 170.11.

LFP Experiments. The nanosecond LFP experiments were performed by using an LKS60 instrument from Applied Photophysics. Pulses of ca. 9 ns and energies of 40 mJ were provided by a Q-switched Nd:YAG laser (Spectron Laser Systems, UK). All experiments were carried out on nitrogen-saturated dichloromethane solutions contained in quartz cells. The transient spectra were obtained by recording the transient decays at different analyzing wavelengths. Typically, the data from four laser pulses at 355 nm were averaged prior to computer processing. In addition, global analysis of the complete kinetic data set of the decays was carried out by using GLint, which is a form of global analysis developed by Applied Photophysics Ltd. that uses the Marquardt–Levenberg algorithm and four order Runge–Kutta numerical integration.¹⁹

Sensitizing experiments were performed with benzophenone in dichloromethane solution. Aliquots of each dissolved pyrazoline were added by using a microliter syringe.

Details of Calculations. All calculations have been done using the Gaussian-98 program.²⁰ Molecular geometries have been fully optimized using the BPW91^{21,22} density functional method with the standard 6-31G(d) basis set.²³ Harmonic vibrational frequencies of all the stationary points have been

(19) Carey, M. *EPA Newsletter* **1994**, 52, 21.

(20) Gaussian 98, Revision A.7: Frisch, M. J.; Trucks, G. W.; Schlegel, H. B.; Scuseria, G. E.; Robb, M. A.; Cheeseman, J. R.; Zakrzewski, V. G.; Montgomery, J. A., Jr.; Stratmann, R. E.; Burant, J. C.; Dapprich, S.; Millam, J. M.; Daniels, A. D.; Kudin, K. N.; Strain, M. C.; Farkas, O.; Tomasi, J.; Barone, V.; Cossi, M.; Cammi, R.; Mennucci, B.; Pomelli, C.; Adamo, C.; Clifford, S.; Ochterski, J.; Petersson, G. A.; Ayala, P. Y.; Cui, Q.; Morokuma, K.; Malick, D. K.; Rabuck, A. D.; Raghavachari, K.; Foresman, J. B.; Cioslowski, J.; Ortiz, J. V.; Stefanov, B. B.; Liu, G.; Liashenko, A.; Piskorz, P.; Komaromi, I.; Gomperts, R.; Martin, R. L.; Fox, D. J.; Keith, T.; Al-Laham, M. A.; Peng, C. Y.; Nanayakkara, A.; Gonzalez, C.; Challacombe, M.; Gill, P. M. W.; Johnson, B.; Chen, W.; Wong, M. W.; Andres, J. L.; Gonzalez, C.; Head-Gordon, M.; Replogle, E. S.; Pople, J. A. Gaussian, Inc., Pittsburgh, PA, 1998. <http://www.gaussian.com>.

(21) Becke, A. D. *Phys. Rev. A* **1988**, 38, 3098.

(22) (a) Wang, Y.; Perdew, J. P. *Phys. Rev. B* **1991**, 44, 13298. (b) Perdew, J. P.; Chevary, J. A.; Vosko, S. H.; Jackson, K. A.; Pederson, M. R.; Singh, D. J.; Fiolhais, C. *Phys. Rev. B* **1992**, 46, 6671.

(17) García-Expósito, E.; Bearpark, M. J.; Ortuño, R. M.; Branchadell, V.; Robb, M. A.; Wilsey, S. *J. Org. Chem.* **2001**, 66, 8811.

(18) (a) Furlani, T. R.; King, H. F. *J. Phys. Chem.* **1985**, 82, 5577. (b) Carlucci, L.; Doubleday, C. Jr.; Furlani, T. R.; King, H. F.; McIver, J. W., Jr. *J. Am. Chem. Soc.* **1987**, 109, 5323.

computed to characterize them as energy minima (all frequencies are real) or transition states (one and only one imaginary frequency). For open-shell systems, a spin-unrestricted formalism has been adopted.

CASSCF²⁴ calculations have been performed for a model system with an active space of six electrons in five orbitals. This active space includes the two open-shell orbitals of the trimethylene moiety and the π orbitals of the nitro group. Minimum energy singlet–triplet crossing points have been located using the methodology developed by Robb et al.²⁵ using state-averaged orbitals with a weighting of 50%/50% to the triplet and singlet states. The CASSCF spin–orbit coupling

(23) (a) Ditchfield, R.; Hehre, W. J.; Pople, J. A. *J. Chem. Phys.* **1971**, *54*, 724. (b) Hehre, W. J.; Ditchfield, R.; Pople, J. A. *J. Chem. Phys.* **1972**, *56*, 2257. (c) Hariharan, P. C.; Pople, J. A. *Theor. Chim. Acta* **1973**, *28*, 213.

(24) Roos, B. O. *Adv. Chem. Phys.* **1987**, *69*, 63.

(25) (a) Ragazos, I. N.; Robb, M. A.; Bernardi, F.; Olivucci, M. *Chem. Phys. Lett.* **1992**, *197*, 217. (b) Bearpark, M. J.; Robb, M. A.; Schlegel, H. B. *Chem. Phys. Lett.* **1994**, *223*, 269.

has been computed using a one-electron approximation with effective charges of 5.6 on O and 3.6 on C.²⁶

Acknowledgment. O.I. thanks the DGR for a pre-doctoral fellowship. Financial support from MCyT (BQU2001-1907) and DURSI (2001SGR-182) and computer time from the Centre de Supercomputació de Catalunya are gratefully acknowledged.

Supporting Information Available: Total energies and geometries of the optimized structures. Crystal data, refinement details, atomic coordinates, thermal parameters, distances, and angles for pyrazoline **3**. ¹H and ¹³C NMR spectra of compounds **3** and **3a**. This material is available free of charge via the Internet at <http://pubs.acs.org>.

JO0342471

(26) Koseki, S.; Schmidt, M. W.; Gordon, M. S. *J. Phys. Chem.* **1992**, *96*, 10768.